

LASER APPLICATIONS AND OTHER TOPICS IN QUANTUM ELECTRONICS

PACS numbers: 42.68.Jg; 42.55.Lt
DOI: 10.1070/QE2007v037n05ABEH013267

On the aerosol backscattering coefficient in atmosphere in the spectral range 9 – 13.5 μm

B.I. Vasil'ev, O.M. Mannoun

***Abstract*. The aerosol backscattering coefficient β_π in a surface atmospheric layer is calculated at the emission lines of NH_3 and CO_2 lasers (9 – 13.5 μm). It is shown that the coefficients β_π at the emission lines of an NH_3 laser (11 – 13.5 μm) are comparable with the coefficients β_π at the emission lines of a CO_2 laser near 10.6 μm. The dependence of β_π on the humidity and type of aerosols is studied. It is also shown that the coefficient β_π in a surface atmospheric layer at the lasing of an NH_3 laser varies from 10^{-10} to 7×10^{-9} cm^{-1} sr^{-1}. The lidar aerosol ratio is calculated as a function of the mean aerosol radius. It is found that this ratio is independent of the particle size for aerosol particles of radius exceeding 40 μm for the 11.7-μm *a*P(4, 0) line of the ammonia laser.**

Keywords: *differential absorption lidar, atmosphere, aerosol, aerosol backscattering coefficient, CO_2 laser, NH_3 laser.*

1. Introduction

The differential absorption lidar based on NH_3 and CO_2 lasers is highly sensitive for probing a large number of substances (Freons, toxins, poisonous materials, etc.) [1]. Simultaneous use of CO_2 (9 – 11 μm) and NH_3 (11 – 13.5 μm) lasers enables this lidar to cover the spectral range of 9 – 13.5 μm [2]. The aerosol backscattering coefficient $\beta_\pi(\lambda)$ of the atmosphere strongly affects the characteristics of differential absorption lidars, namely, the signal-to-noise ratio and the accuracy of measuring the concentration of gases, especially in the region of inhomogeneities of the aerosol distribution [3, 4].

The profile of $\beta_\pi(\lambda)$ at CO_2 laser lines was studied in [5 – 10], but investigations were hampered by a large spread of experimental data obtained by various authors and the variability of structure of aerosols. It was shown in [9] that at β_π a wavelength of 10.6 μm varies from 10^{-6} m^{-1} sr^{-1} (in the planetary boundary layer) to 10^{-11} m^{-1} sr^{-1} (in the stratosphere). However, the values of β_π in free troposphere are very low ($10^{-10} - 10^{-12}$ m^{-1} sr^{-1}).

B.I. Vasil'ev, O.M. Mannoun P.N. Lebedev Physics Institute, Russian Academy of Sciences, Leninsky prosp. 53, 119991 Moscow, Russia; e-mail: bvasil@sci.lebedev.ru

Received 16 February 2006, revision received 13 July 2006
Kvantovaya Elektronika **37** (5) 500 – 502 (2007)
Translated by Ram Wadhwa

Experimental investigations performed in [5] show that β_π varies from 4×10^{-8} m^{-1} sr^{-1} to 2×10^{-7} m^{-1} sr^{-1} at CO_2 laser lines. Measurements were made under climatic conditions of a desert on a horizontal path at the sea level. Measurements at 19 spectral lines in the spectral interval 9.2 – 10.7 μm show that β_π has two maxima, the first one at the 10R(20) line (10.247 μm) and the second one at 9P(40) line (9.733 μm).

In this paper, we studied theoretically the aerosol backscattering coefficient β_π in a surface layer of atmosphere at the $NH_3 - CO_2$ laser lines (9 – 13.5 μm). The calculations were based on the Mie theory [11, 12] for three types of aerosols (urban, sea and continental) for a relative humidity of 20 % – 95 %.

2. Theoretical model

According to the Mie theory [11, 12] of scattering of electromagnetic waves by aerosol particles, the aerosol backscattering coefficient β_π and the extinction coefficient α are

$$\beta_\pi(m, \lambda) = \int_0^\infty \pi r^2 Q_{\text{scat}}(x, m, \lambda) f(r) \mathrm{d}r, \tag{1}$$

$$\alpha(m, \lambda) = \int_0^\infty \pi r^2 Q_{\text{ext}}(x, m, \lambda) f(r) \mathrm{d}r, \tag{2}$$

where r is the particle radius; $x = 2\pi r/\lambda$ is the relative particle size; $f(r)$ is the size distribution function of aerosol particles; m is the refractive index of aerosol ($m = n - \mathrm{i}\chi$); Q_{scat} and Q_{ext} are the backscattering and extinction coefficients respectively, which are expressed in terms of the Mie intensity functions and the relative particle size x.

It is known [13 – 15] that the size and shape of atmospheric aerosols are extremely variable in space and time. These particles are usually divided into three groups depending on their size [14]: fine (0.002 – 0.1 μm), medium (0.1 – 1 μm) and coarse (larger than 1 μm) aerosols. The main parameters of aerosols are their complex refractive index and size distribution function. The complex refractive index is determined by the chemical composition of the aerosol. The size distribution function $f(r)$ of aerosol particles is often approximated by the three-mode logarithmically normal distribution [15]

$$f(r) = \sum_{i=1}^{3} \frac{N_0^{(i)}}{\sqrt{2\pi} r \ln \sigma^{(i)}} \exp\left\{ -\frac{1}{2} \left[\frac{\ln(r/r_{\text{m}}^{(i)})}{\ln \sigma^{(i)}} \right]^2 \right\}, \tag{3}$$

where $r_m^{(i)}$ is the mean radius of the ith mode aerosol particles; $\sigma^{(i)}$ is the ith mode distribution width; and $N_0^{(i)}$ is the integrated concentration of the ith mode aerosol particles.

Variation of humidity due to coagulation and condensation processes affects not only the refractive index of the aerosol, but also its size. Therefore, we took into account in calculations the increase in the particle radius r as a function of humidity, which is described by the expression [14]

$$\frac{r}{r_0} = (1 - H)^{-0.25}, \quad (4)$$

where H is the relative humidity ($0.2 < H < 0.99$); r_0 is the radius of a dry particle.

We used in calculations the complex refractive index profile of the aerosol from [14]. Figures 1 and 2 show the real and imaginary parts of the complex refractive index of aerosols that are typical of the surface atmospheric layer. One can see from Fig. 2 that there are three absorption bands: the intense band at 9.4 μm and two relatively weak bands at 11.4 and 12.6 μm. With increasing humidity, the real part of the refractive index of aerosols (see Fig. 1) decreases and tends to the real part of the refractive index of water. To reduce the calculation time, especially in the case of large aerosole particles, algorithms proposed in [16] were used.

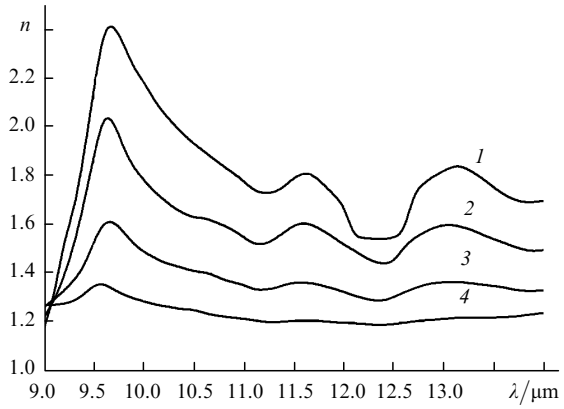

Figure 1. Dependence of the real part of complex aerosol refractive index [14] on λ for a relative humidity of 20 %–25 % (*1*), 35 %–45 % (*2*), 75 %–85 % (*3*) and 90 %–95 % (*4*).

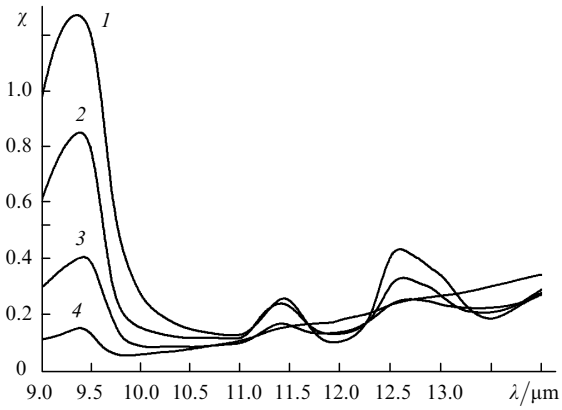

Figure 2. Dependence of the imaginary part of complex aerosol refractive index [14] on λ for a relative humidity of 20 %–25 % (*1*), 35 %–45 % (*2*), 75 %–85 % (*3*) and 90 %–95 % (*4*).

3. Discussion

Table 1 presents the main parameters of distribution (3) for three types of aerosols: urban, sea and continental [15]. The first (fine disperse) mode is not taken into account because its effect on β_π is insignificant, especially in the IR spectral region.

Table 1.

Type of aerosol	$N_0^{(2)}$/ cm^{-3}	$r_m^{(2)}$/μm	$\ln\sigma^{(2)}$	$N_0^{(3)}$/ cm^{-3}	$r_m^{(3)}$/μm	$\ln\sigma^{(3)}$
Urban	20000	0.04	0.63	6	0.63	0.77
Sea	400	0.05	0.68	3.8	0.65	0.74
Continental	4000	0.03	0.74	2.1	0.4	0.81

Figure 3 shows the profiles of coefficient $\beta_\pi(\lambda)$ normalised to β_π (11.7 μm) for urban aerosol for different relative humidities. One can see that the values of β_π at ammonia laser lines are comparable with β_π for CO_2 laser lines at ~10.6 mm, but about half or one-third of the value of β_π at CO_2 laser lines at ~9.6 μm. One can also see that as the relative humidity increases, the values of β_π at wavelengths exceeding 12 μm become larger than the values for CO_2 laser lines at ~10.6 μm, but remain smaller than β_π for CO_2 laser lines at ~9.6 μm. This means that the lidar parameters at the ammonia and CO_2 laser lines at ~10.6 μm are comparable.

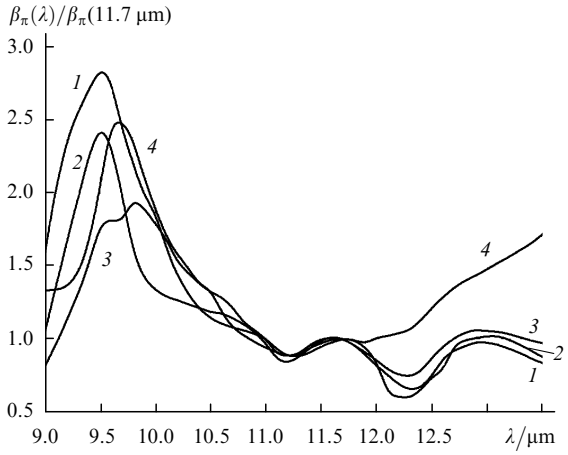

Figure 3. Profiles of the coefficient $\beta_\pi(\lambda)$ normalised to β_π(11.7 μm) for urban aerosol for a relative humidity of 20 %–25 % (*1*), 35 %–45 % (*2*), 75 %–85 % (*3*) and 90 %–95 % (*4*).

Model calculations showed that the coefficients β_π at the ammonia laser lines vary from 10^{-10} to 7×10^{-9} cm^{-1} sr^{-1}, the higher values of β_π corresponding to the urban aerosol and the lower ones to the continental aerosol, which is obviously related to the mean radius of aerosols (see Table 1). In all the cases, a minimum value of β_π is observed at $\lambda \sim 12.3$ μm except when the relative humidity amounts to 90 %–95 % and the minimum is displaced towards $\lambda \sim 11.2$ μm. Such a behaviour of $\beta_\pi(\lambda)$ can be explained by a significant role of water whose refractive index has a minimum at $\lambda \sim 11.2$ μm.

Figure 4 shows the dependence of the lidar ratio $L = \alpha/\beta_\pi$ on the mean aerosol radius r_m for three wavelengths (9.6, 10.6 and 11.7 μm). One can see that with

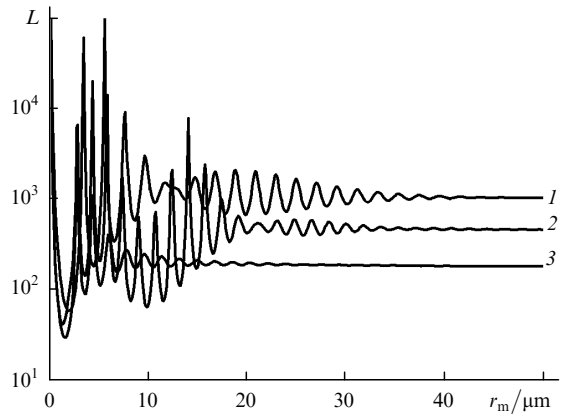

Figure 4. Lidar ratio L as a function of the mean radius r_m of aerosol particles for wavelengths 11.7 μm ($m = 1.206 - i \times 0.17$) [curve (*1*)], 10.6 μm ($m = 1.237 - i \times 0.087$) [curve (*2*)] and 9.6 μm ($m = 1.357 - i \times 0.089$) [curve (*3*)].

increasing r_m, the lidar ratio tends to a constant value $L_0(\lambda)$ which is attained for a certain value of $r_0(\lambda)$. The values of L_0 are defined by the laws of geometrical optics upon reflection at the interface between two media, i.e., by the refractive index and the absorption coefficient. It can also be seen that $r_0 = 20$, 35 and 40 μm for $\lambda = 9.6$, 10.6 and 11.7 μm, respectively. Such a behaviour of the $L_0(\lambda)$ dependence is extremely important for probing large aerosols since it can be used for obtaining the profiles of aerosol extinction and scattering coefficients directly from lidar signals with a high degree of precision.

4. Conclusions

Our investigations show that the characteristics of lidars at the ammonia and CO_2 laser lines of about 10.6 μm are comparable, and the parameters of the ammonia lidar for a high relative humidity (90 % – 95 %) improve and approach those of the lidars at CO_2 laser lines at about 9.6 μm. The aerosol back scattering coefficient at the ammonia laser line in the surface atmospheric layer varies from 10^{-10} to 7×10^{-9} cm^{-1} sr^{-1}, depending on the type of aerosol and the state of the atmosphere.

References

1. Vasil'ev B.I., Mannoun O.M. *Kvantovaya Elektron.*, **35**, 523 (2005) [*Quantum Electron.*, **35**, 523 (2005)].
2. Vasil'ev B.I., Zheltukhin A.A., Mannoun O.M. *Kratk. Soobshch. Fiz. FIAN*, **7**, 22 (2004).
3. Zuev V.E., Zuev V.V. *Distantsionnoe opticheskoe zondirovanie atmosphery* (Remote Optical Sensing of Atmosphere) (St. Petersburg: Gidrometeoizdat, 1992).
4. Measures R.M. *Laser Remote Sensing. Fundamentals and Applications* (New York: JW & Sons Inc., 1984).
5. Ben-David A. *Appl. Opt.*, **38** (12), 2616 (1999).
6. Walter D.P. et al. *Appl. Opt.*, **25** (15), 2506 (1986).
7. Petheram J.C. *Appl. Opt.*, **20** (22), 3941 (1981).
8. Walter D.P. et al. *Appl. Opt.*, **25** (15), 2506 (1986).
9. Kent G.S. et al. *Appl. Opt.*, **22** (11), 1666 (1983).
10. Jennings S.G. *Appl. Opt.*, **25** (15), 2499 (1986).
11. Van de Hulst H.C. *Light Scattering by Small Particles* (New York: JW & Sons Inc., 1957).
12. Borhn C.F., Huffman D.R. *Absorption and Scattering of Light by Small Particles* (New York: JW & Sons Inc., 1983).
13. Zuev V.E., Kabanov M.V. *Optika atmosphernogo aerosolya* (Optics of the Atmospheric Aerosol) (Leningrad: Gidrometeoizdat, 1987).
14. Ivlev V.E., Andreev S.D. *Opticheskie svoistva atmosfernykh aerozolei* (Optical Properties of Atmospheric Aerosols) (Leningrad: Izd. LGU, 1986).
15. Jaenicke R., in *Aerosol Climate Interaction* (New York: Acad. Press, 1993) p. 233.
16. Wiscombe W.J. *Appl. Opt.*, **19** (9), 1505 (1980).